

GEOMETRIC MODELLING AND PHOTOGRAMMETRIC PROCESSING OF HIGH-RESOLUTION SATELLITE IMAGERY

Xutong Niu, Jue Wang, Kaichang Di, Jin-Duk Lee, Ron Li

Mapping and GIS Laboratory, CEEGS, The Ohio State University
 470 Hitchcock Hall, 2070 Neil Avenue, Columbus, OH 43210-1275 USA
 Email: {niu.9, di.2, wang.813, di.2, lee.2322, li.282}@osu.edu

Commission IV, WG IV/7

KEY WORDS: Photogrammetry, High Resolution, Adjustment, Accuracy, Orthoimage, DEM.

ABSTRACT:

The latest generation of high-resolution commercial imaging satellites, such as IKONOS and QuickBird, has opened a new era of earth observation and digital mapping. This paper presents the geometric modeling principles and photogrammetric processing methods involved in high-precision mapping using stereo IKONOS and QuickBird images. First, the imaging geometry and systematic errors in the Rational Function-based sensor model are described. Then the results of a comparison study of IKONOS and QuickBird geopositioning accuracy improvement in which different adjustment models, as well as different number and configuration of ground control points, are presented. Results indicate that a simple adjustment model (e.g., Affine or Scale & Translation) is effective for elimination of the systematic errors found in vendor-provided RFCs (Rational Function Coefficients) and for improvement of 3D geopositioning accuracies to a 1-2m level for IKONOS images and a 0.6-1m level for QuickBird images. For coastal mapping purposes, a semi-automatic 3D shoreline extraction method is proposed. In this method, a 2D shoreline is extracted by manual digitizing on one QuickBird image; then corresponding shoreline points on the other image of the stereo pair are automatically extracted by image matching. The 3D shoreline is computed using photogrammetric triangulation with the improved geometric model.

INTRODUCTION

Since September 24, 1999, when the IKONOS satellite was successfully launched, high-resolution (meter to sub-meter pixel resolution) satellite imagery have been rapidly incorporated into the applications of municipal planning, transportation, mining, remote area mapping, agriculture, environmental investigation and disaster response. Digital satellite imagery not only provides substantial high quality data for mapping, inventorying, monitoring, and surveying, but also allows for digital data processing and interpretation. The latest generation of high-resolution commercial satellites, such as IKONOS and QuickBird, has opened a new era of earth observation and digital mapping. This paper presents the geometric modeling principles and photogrammetric processing methods involved in high-precision mapping using stereo IKONOS and QuickBird images.

Space Imaging Corporation provides IKONOS imagery with different processing levels and corresponding positioning accuracy. These include the Geo, Reference, Pro, Precision and Precision Plus products (Space Imaging, 2002). The IKONOS imaging system simultaneously collects 0.8 meter-resolution stereo panchromatic and 4 meter multispectral images. Provided by DigitalGlobe Inc., QuickBird imagery is the highest-resolution satellite imagery now commercially available. The QuickBird imaging system simultaneously collects 67-72 centimeter-resolution stereo panchromatic and 2.44-2.88 meter multi-spectral images. Using different processing levels, DigitalGlobe provides three types of QuickBird products for the same scene including basic, standard, and orthorectified image products (DigitalGlobe, 2002). Table 1 lists the associated accuracies of different

IKONOS and QuickBird image products. Table 2 shows some technical specifications of IKONOS and QuickBird satellites (Space Imaging, 2002 and DigitalGlobe, 2002).

| IKONOS | | QuickBird | |
|----------------|----------|-----------------------------|-----------------------------|
| Products | Accuracy | Product | Accuracy |
| Geo | 25.0 m | Basic | 14 m |
| Reference | 11.8 m | Standard | 14 m |
| Pro | 4.8 m | Orthorectified (1:25,000) | 7.7 m |
| Precision | 1.9 m | Orthorectified (1:12,000) | 6.2 m |
| Precision Plus | 0.9 m | Orthorectified (Customized) | depend on qualities of GCPs |

Table 1. Accuracies of IKONOS and QuickBird image products

Highly accurate image products, such as IKONOS Precision or QuickBird Orthorectified, cost much more than lower level products. Therefore, it is desirable to use the lower-cost image products while achieving accuracies comparable to those of the more expensive ones. A number of investigations on the accuracy attainable by various methods of photogrammetric processing of IKONOS and QuickBird imagery have been reported (Li, 1998; Zhou and Li, 2000; Tao and Hu, 2001; Fraser and Hanley, 2003; Toutin, 2003). An overview of IKONOS mapping accuracy is given in Grodecki and Dial (2001). However, there is a need for additional literature on the processing and geopositioning analysis of QuickBird imagery.

| Specifications | IKONOS II Satellite | QuickBird II Satellite |
|-----------------------|--|--|
| First Launch Date | September 24, 1999 | October 18, 2001 |
| Orbit | 98.1 degree, sun synchronous | 97.2 degree, sun synchronous |
| Speed on Orbit | 7.5 km / second | 7.1 km / second |
| Orbit Time | 98 minutes | 93.5 minutes |
| Altitude | 681 kilometers | 450 kilometers |
| Pixel Resolution | Nadir: 0.82 meters panchromatic 3.2 meters multispectral 26° Off-Nadir: 1.0 meter panchromatic 4.0 meters multispectral | Nadir: 0.61 meters panchromatic 2.44 meters multispectral 25° Off-Nadir: 0.72 meters panchromatic 2.88 meters multispectral |
| Image Swath | 11.3 km at nadir 13.8 km at 26° off-nadir | 16.5 kilometers at nadir |
| Equator Crossing Time | Nominally 10:30 a.m. solar time | 10:30 a.m. (descending node) |
| Revisit Time | Approximately 3 days at 1-meter resolution, 40° latitude | 1-3.5 days depending on latitude (30° off nadir) |
| Dynamic Range | 11 bits per pixel | 11 bits per pixel |
| Image Bands | Panchromatic, blue, green, red, near infrared | Panchromatic, blue, green, red, near infrared |

Table 2. Technical specifications of IKONOS and QuickBird satellites (Space Imaging, 2002; Digital Globe, 2002)

RATIONAL FUNCTIONS

Both IKONOS and QuickBird stereo images are provided with Rational Function Coefficients (RFCs). As an alternative to a physical camera model, the rational function (RF) describes the transformation between the image and object spaces. The rational function transforms a point in the object space (X, Y, Z) into its corresponding image point (i, j) through a ratio of the two polynomials shown in Equation (1),

$$\begin{cases} i = \frac{P_1(X, Y, Z)}{P_2(X, Y, Z)} \\ j = \frac{P_3(X, Y, Z)}{P_4(X, Y, Z)} \end{cases} \quad (1)$$

where the polynomial P_i ($i=1, 2, 3,$ and 4) has the following general form:

$$\begin{aligned} P(X, Y, Z) = & a_1 + a_2X + a_3Y + a_4Z + a_5XY + a_6XZ + a_7YZ + a_8X^2 \\ & + a_9Y^2 + a_{10}Z^2 + a_{11}XYZ + a_{12}X^3 + a_{13}XY^2 + a_{14}XZ^2 \\ & + a_{15}X^2Y + a_{16}Y^3 + a_{17}YZ^2 + a_{18}X^2Z + a_{19}Y^2Z + a_{20}Z^3 \end{aligned} \quad (2)$$

This is a third-order rational function with a 20-term polynomial that transforms a point from the object space to the image space. Substituting P_i s in Equation (1) with the polynomials in Equation (2) and eliminating the first coefficient in the denominator, we have a total of 39 RF coefficients in each equation: 20 in the numerator and 19 in the denominator. Since each GCP produces two equations, at least 39 GCPs are required to solve for the 78 coefficients.

Although they do not describe sensor parameters explicitly, RFs are simple to implement and perform transformations very rapidly. They can be used effectively for feature extraction, terrain model generation, and orthorectification. Generally, RF coefficients are estimated without the aid of ground control (Tao and Hu, 2001; Di et al., 2001). Thus, some biases inherent in RFs may not be corrected, and may be reflected in the geopositioning accuracy. Li et al. (2003) found a systematic error of 6 meters between RF-derived coordinates and the ground truth. A similar result was reported in Fraser and Hanley (2003). It is desirable that such errors in the image products be reduced or eliminated by users employing relatively simple methods that can be used for many different applications that require higher mapping accuracy.

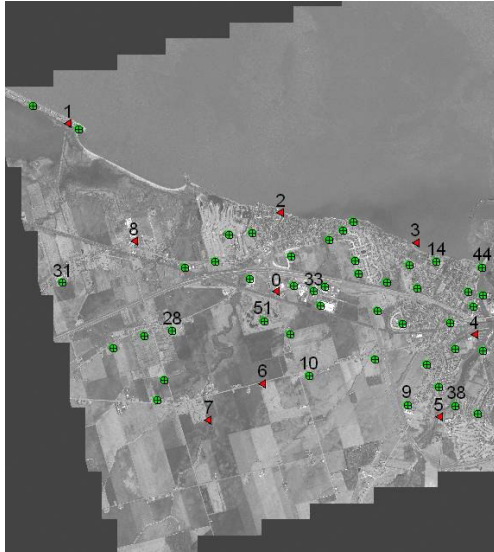
In this research, a pair of IKONOS stereo Geo product images and a pair of QuickBird basic product stereo images were used to evaluate methods for the improvement of geopositioning accuracy based on RF models. Three-dimensional shorelines were also extracted from both stereo pairs for coastal modeling.

DATA

The IKONOS stereo images used in this experiment were taken in May 2002 in a Lake Erie coastal area. RFCs of each image were supplied by Space Imaging Corp. The QuickBird stereo images (Panchromatic and Multispectral) used in this experiment were taken in September 2003 in southern Tampa Bay, Florida. RFCs of the imagery were supplied by DigitalGlobe, Inc. The GCPs (ground control points) used in this experiment were obtained from GPS surveys conducted in Ohio in March 2000 and in Florida in November 2002, respectively. Check points (CKPs) are those points obtained from high quality aerial photogrammetric triangulations of overlapped aerial images taken in the same areas. The accuracy of these GCPs is 6 cm in the horizontal and 9 cm in the vertical directions. The accuracy of the CKPs is estimated as 0.5 m. Figure 1 gives the distribution of GCP and CKP points in the forward-looking images of both stereo pairs.

The image coordinates of the GCP and CKP points were measured manually. Ground coordinates of the measured points were calculated using the RFCs supplied with the data. After registering both sets of ground coordinates within the same reference system (for example, the QuickBird images are based on State Plane, NAD 83, Florida West), differences between the RFC-derived coordinates of the control points and their GPS-surveyed coordinates were calculated. Figure 2 shows such differences in the QuickBird image measurements. The display in

Figure 2 is exaggerated 50 times for better visualization. From Figure 2, it can be seen that the dominant errors are systematic and exist mainly in the north-east direction. The RMS errors for both QuickBird panchromatic and multispectral pairs are shown in Table 3. For similar results using IKONOS data, refer to Di et al. (2002).



(a) IKONOS image



(b) QuickBird image

Figure 1. Distribution of GCPs (red triangles) and CKPs (green circles)

| Image Type | X | Y | Z |
|--------------------------------------|--------|--------|---------|
| Errors in panchromatic pair (meter) | 8.846m | 8.738m | 12.667m |
| Errors in multispectral pair (meter) | 8.594m | 7.498m | 32.296m |

Table 3. Differences (RMS) computed from GCPs and RFC-derived ground points

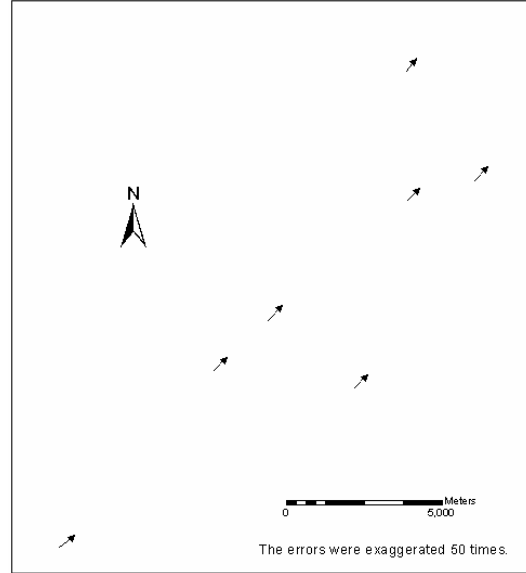


Figure 2. Differences between the RFC-derived and GPS-surveyed ground coordinates of GCP points (panchromatic QuickBird stereo images)

ACCURACY IMPROVEMENT

In general, there are two ways to improve the accuracy of RFC-derived ground coordinates (Di et al., 2003a; Li et al., 2003). The first is to refine the RFCs based on a large number of GCPs (more than 39 GCPs are required for the third-order RF). This method is theoretically applicable, but not practical where large numbers of such GCPs are not available. The second approach refines the ground coordinates calculated from the RFs using a polynomial correction in either the image space or object space. This method requires significantly fewer GCPs than the first approach, and has the advantages of simplicity and efficiency. A number of publications have reported results using variations of this approach (Grodecki and Dial, 2003; Di et al., 2003b).

In this research, four models are evaluated for their ability to improve accuracies in both the object space and image space: 1) translation, 2) scale and translation, 3) affine, and 4) a second-order polynomial (Table 4). For each model in object space, RF-based triangulation (Di et al., 2001; 2003a) is applied to calculate the ground coordinates (X, Y, Z). Since the correct coordinates (X', Y', Z') of the GCPs are known, three equations can be established in accordance with the model equations in Table 4. Using all available GCPs (usually more than the minimum number required), over-determined equation systems can be set up to compute the optimal estimates of the transformation parameters by a least-squares adjustment. The transformation parameters can be used to compute the improved coordinates of other points. CKPs are used to assess the appropriateness of the models. The root mean square error (RMSE) of each model is calculated based on differences between RF-derived and known coordinates of the CKPs.

In object space, the translation model adds a shift vector (a_0, b_0, c_0) to the ground coordinates (X, Y, Z) computed from the RFCs to

achieve the improved coordinates (X' , Y' , Z'). It requires at least one GCP. The second model uses three additional scale factors (a_1 , b_1 , c_1) to correct non-homogeneous scale distortions. An affine transformation and a second-order polynomial transformation are applied to the third and fourth models, respectively. In image space, the image coordinates (I , J) are improved by four similar models to compute the corrected image coordinates (I' , J'). However, these models are simplified by dropping the parameters associated with the third dimension. The implementation and assessment processes are the same as those in the object space.

| | ID | Adjustment Models | Min. No. of GCPs |
|--------------|----|---|------------------|
| Object Space | 1 | Translation $X' = a_0, Y' = b_0, Z' = c_0$ | 1 |
| | 2 | Scale and Translation $X' = a_0 + a_1X$ $Y' = b_0 + b_1Y$ $Z' = c_0 + c_1Z$ | 2 |
| | 3 | Affine $X' = a_0 + a_1X + a_2Y + a_3Z$ $Y' = b_0 + b_1X + b_2Y + b_3Z$ $Z' = c_0 + c_1X + c_2Y + c_3Z$ | 4 |
| | 4 | Second-order Polynomial $X' = a_0 + a_1X + a_2Y + a_3Z + a_4XY + a_5XZ + a_6YZ + a_7X^2 + a_8Y^2 + a_9Z^2$ $Y' = b_0 + b_1X + b_2Y + b_3Z + b_4XY + b_5XZ + b_6YZ + b_7X^2 + b_8Y^2 + b_9Z^2$ $Z' = c_0 + c_1X + c_2Y + c_3Z + c_4XY + c_5XZ + c_6YZ + c_7X^2 + c_8Y^2 + c_9Z^2$ | 10 |
| Image Space | 1 | Translation $I' = a_0, J' = b_0$ | 1 |
| | 2 | Scale and Translation $I' = a_0 + a_1I$ $J' = b_0 + b_1J$ | 2 |
| | 3 | Affine $I' = a_0 + a_1I + a_2J$ $J' = b_0 + b_1I + b_2J$ | 3 |
| | 4 | Second-order Polynomial $I' = a_0 + a_1I + a_2J + a_3II + a_4I^2 + a_5J^2$ $J' = b_0 + b_1I + b_2J + b_3II + b_4I^2 + b_5J^2$ | 6 |

Table 4. Adjustment models defined in object and image space

The experiment starts with each model using the minimum number of GCPs (see Table 4). Additional GCPs are then added to improve accuracy. Various combinations of the number and distribution of GCPs are also tested to determine the effectiveness of different configurations.

| Method | No. GCPs | GCP Distribution | RMSE (m) | | | Maximum Difference (m) | | |
|-----------------------|----------|--------------------|----------|-------|-------|------------------------|-------|-------|
| | | | X | Y | Z | X | Y | Z |
| Translation | 1 | 1 | 1.000 | 0.733 | 2.264 | 3.424 | 2.079 | 4.606 |
| Scale and Translation | 2 | Along Track 3-9 | 1.118 | 0.693 | 2.187 | 3.859 | 1.816 | 5.524 |
| | | Cross Track 3-8 | 1.032 | 0.822 | 2.222 | 3.673 | 2.867 | 5.984 |
| | 4 | 1-3-5-7 | 1.192 | 0.626 | 2.008 | 3.824 | 1.650 | 4.943 |
| | 6 | 0-2-4-5-6-8 | 1.068 | 0.712 | 1.941 | 3.926 | 2.034 | 4.639 |
| Affine | 4 | 1-3-5-7 | 1.525 | 0.645 | 3.217 | 4.871 | 1.488 | 5.850 |
| | 6 | 1-3-4-5-7-8 | 1.179 | 0.736 | 1.678 | 4.498 | 2.098 | 4.195 |

Table 5. Accuracy of ground points improved by three object space-based models in IKONOS stereo images

IMPROVEMENT RESULTS AND DISCUSSION

Tables 5 and 6 show improvements in accuracy achieved by the three different methods performed in the object space for both IKONOS and QuickBird stereo images, respectively. It should be noted that the minimum number of control points is not met with the available GCPs for the second-order polynomial model. In the GCP distribution column of both tables, each digit (from 0 to 8) represents a control point ID (as indicated in Figure 1). Improvement results for the models performed in the image space are summarized in Tables 7 and 8. A discussion of the results of each method is given below.

| Method | No. GCPs | GCP Distribution | RMSE (m) | | | Maximum Difference (m) | | |
|-----------------------|----------|--------------------|----------|-------|-------|------------------------|-------|-------|
| | | | X | Y | Z | X | Y | Z |
| Translation | 1 | 1 | 0.437 | 0.631 | 0.815 | 0.719 | 1.003 | 1.361 |
| Scale and Translation | 2 | Along Track 2-7 | 0.843 | 1.152 | 1.131 | 1.283 | 2.286 | 1.553 |
| | | Cross Track 3-6 | 0.308 | 1.071 | 0.912 | 0.383 | 1.384 | 1.328 |
| | 4 | 0-3-5-7 | 0.272 | 0.612 | 0.523 | 0.396 | 0.724 | 0.650 |
| | 6 | 5-6-3-7-2-0 | 0.447 | 0.243 | 0.624 | 0.447 | 0.243 | 0.624 |
| Affine | 4 | 0-3-5-7 | 0.206 | 0.794 | 0.809 | 0.308 | 1.130 | 0.955 |
| | 6 | 5-6-3-7-2-0 | 0.280 | 0.570 | 0.429 | 0.280 | 0.570 | 0.429 |

Table 6. Accuracy of ground points improved by three object space-based models for QuickBird stereo images

| Method | No. GCPs | GCP Distribution | RMSE (m) | | | Maximum Difference (m) | | |
|-------------------------|----------|--------------------|----------|-------|-------|------------------------|-------|-------|
| | | | X | Y | Z | X | Y | Z |
| Translation | 1 | 5 | 1.365 | 0.631 | 1.355 | 3.702 | 1.530 | 3.219 |
| Scale and Translation | 2 | Along Track 1-3 | 1.202 | 1.214 | 2.855 | 3.856 | 2.577 | 7.786 |
| | | Cross Track 5-1 | 1.318 | 0.653 | 1.272 | 4.099 | 1.385 | 2.821 |
| | 4 | 2-3-5-6 | 1.366 | 0.658 | 1.163 | 4.017 | 1.531 | 2.757 |
| | 6 | 1-3-4-5-7-8 | 1.350 | 0.651 | 1.233 | 4.225 | 1.448 | 2.872 |
| Affine | 4 | 1-3-5-7 | 1.373 | 0.500 | 1.288 | 3.888 | 1.170 | 3.006 |
| | 6 | 1-3-4-5-7-8 | 1.431 | 0.597 | 1.137 | 4.230 | 1.502 | 2.787 |
| Second-Order Polynomial | 6 | 0-2-3-4-6-8 | 1.524 | 1.287 | 1.537 | 5.915 | 5.167 | 4.505 |
| | 10 | evenly | 1.366 | 0.557 | 1.362 | 3.681 | 1.531 | 3.860 |

Table 7. Accuracy of ground points improved by four image space-based models for IKONOS stereo images

Translation Model: This model offers a simple way to improve accuracy by a translation in either object or image space. Using one GCP, reasonable accuracies can be achieved. For IKONOS images, RMSE generally is less than 1 m in the horizontal and 2.5

m in the vertical; while for QuickBird images, RMSE is less than 1 m in horizontal and 1.2 m in the vertical. The level of accuracy has no apparent relationship to the location of the GCP used. However, since only one GCP is used, the quality of the GCP is critical to the final result.

| Method | No. GCPs | GCP Distribution | | RMSE (m) | | | Maximum Difference (m) | | |
|-------------------------|----------|------------------|-------------|----------|-------|-------|------------------------|-------|-------|
| | | | | X | Y | Z | X | Y | Z |
| Translation | 1 | 1 | | 0.619 | 0.669 | 0.425 | 0.983 | 0.960 | 0.726 |
| Scale and Translation | 2 | Along Track | 1-7 | 0.942 | 0.689 | 0.494 | 1.396 | 1.266 | 0.811 |
| | | | Cross Track | 3-6 | 0.555 | 1.045 | 0.445 | 0.943 | 1.357 |
| | 4 | 0-3-5-7 | | 0.291 | 0.591 | 0.378 | 0.398 | 0.700 | 0.585 |
| | 6 | 5-6-3-7-2-0 | | 0.451 | 0.241 | 0.175 | 0.451 | 0.241 | 0.175 |
| Affine | 4 | 0-3-5-7 | | 0.284 | 0.789 | 0.362 | 0.327 | 0.895 | 0.539 |
| | 6 | 5-6-3-7-2-0 | | 0.401 | 0.463 | 0.174 | 0.401 | 0.463 | 0.174 |
| Second-Order Polynomial | 6 | 5-6-3-7-1-0 | | 0.530 | 0.706 | 0.342 | 0.530 | 0.706 | 0.342 |

Table 8. Accuracy of ground points improved by four image space-based methods in QuickBird stereo images

Scale and Translation Model: The scale and translation model has additional scaling factors in the coordinate axis directions. At least two GCPs are necessary for this model. In the object space, if these two GCPs used are distributed in the cross-track direction, the computed RMSEs of the ground points are relatively smaller than if they are distributed in the along-track direction. This trend is consistent with the results achieved using simulated IKONOS images (Zhou and Li, 2000). The RMSEs calculated by using the model in image space with two GCPs shows similar results associated with the GCP distribution. In order to increase redundancy, more GCPs should be used. With four evenly distributed GCPs (see 1357 in Table 5 and 0357 in Table 6 – close to four corners), the result is improved (for QuickBird images, the RMSE is less than 62 cm in the horizontal and 53 cm in the vertical) in both object and image spaces. With six GCPs, a more consistent and better result (for QuickBird images, RMSE is less than 50 cm in the horizontal and 63 cm in vertical directions) is shown using the method in both object and image spaces.

Affine Model: The affine model offers the capability of considering affinity. However, the additional affine parameters and GCPs do not generate an improvement over the result from the scale and translation model when used in the object space. In the image space, however, a comparable result is obtained by using six GCPs (for QuickBird images, to less than 50 cm in the horizontal and 20 cm in vertical).

Second-Order Polynomial: The addition of the second-order parameters requires the use of a larger number of GCPs. Therefore, it is only applied to image space, where the model uses six GCPs. No significant improvements are found in comparison to the other three models. In general, high-order polynomials are

very sensitive and require a large number of GCPs and a very even GCP distribution. The second-order polynomial model does not exhibit convincing advantages over other models.

The accuracy of the U.S. Geological Survey (USGS) 1:24,000 scale topographic map is approximately 12.2 meters. The National Oceanic and Atmospheric Administration /National Geodetic Survey (NOAA/NGS) 1:5,000 Coastal Topographic Survey Sheet (T-Sheet) is accurate to within approximately 2.5 meters (Li et al., 2001). Thus, ground points derived from IKONOS one-meter and QuickBird sub-meter panchromatic stereo images are appropriate for updating features in both the USGS 1:24,000 topographic maps and the NOAA/NGS T-Sheets. Furthermore, both kinds of stereo images can be used for high-resolution coastal mapping.

APPLICATION: 3-D SHORELINE EXTRACTION

A semi-automatic method is applied to extract a 3-D shoreline from QuickBird stereo images. To extract the 3-D shoreline, shoreline image coordinates must be obtained in both images of a stereo pair. If performed manually, this process is very labor intensive and time consuming. It is difficult to find conjugate points on the shoreline in areas where the shoreline does not have much change in shape and/or the background does not have sufficient texture information. In this research, a semiautomatic method was developed to solve these problems.



Figure 3. 3-D shoreline overlapping with QuickBird orthophoto

Since QuickBird stereo images are not resampled by the vendor using epipolar geometry, a second-order polynomial relationship between two stereo images was set up first. Through this relationship, the position of the conjugate point of a shoreline vertex in one stereo image can be approximately located in the other stereo image within a close neighborhood. The closeness of the transformed point in this experiment is around 4 pixels in both the x and y directions. Then, an area-based matching using

normalized correlation coefficients was performed in the raw images. Based on ESRI ArcObjects and Microsoft.Net C# programming language, a shoreline extraction system was developed to aid in shoreline digitizing, point matching, 3D coordinate calculating, and result checking. 3-D coordinates of the shoreline can be calculated from the matched image points in the stereo images using RFCs supplied by the vendor (Li et al., 2003). The refinement of the calculated coordinates was done by applying a translation model in the object space as discussed above. A transformation was carried out to convert the geographic coordinates (latitude, longitude) into State Plane coordinates. Figure 3 shows the calculated shoreline from the QuickBird panchromatic stereo images along with the orthophoto generated automatically using the OrthoBase module of ERDAS Imagine 8.6. It can be seen that the semiautomatic result fits very well with the orthophoto.

CONCLUSIONS

This paper presents the experimental results of a study on accuracy improvement of ground points determined by IKONOS and QuickBird images using GCPs and different transformation models in both object and image spaces. Different methods and GCP distribution patterns are tested. Complete tables of computational results are given for discussion as well as supplying the reader with information for their own analysis. As an application of the method, a 3-D shoreline was extracted from QuickBird panchromatic stereo images. We can draw the following conclusions based on the above experimental results.

In general, there are no significant differences in the results from using the different models in the object or image space, although the affine and higher-order polynomial models in the image space require fewer GCPs than the models in object space. The models are generally more stable in the image space, considering the maximum differences observed. The quality of the IKONOS and QuickBird images is excellent. Using a simple translation model and one GCP we can correct the majority of errors and achieve a good result. It is recommended that a scale and translation model or an affine model with four to six well-distributed GCPs be used to achieve a high level of accuracy. These methods seem to be most practical for use in mapping applications.

The objects chosen in this study are general image features such as road intersections, building corners, and other objects distinguished in the coastal area. The precision of the image point measurement is about one-half to one pixel. The accuracy improvement method was then applied to 3D shoreline extraction. The derived 3D shoreline from QuickBird stereo images reached a ground accuracy of about 0.65 meters, which is well beyond the accuracy of the NOAA/NGS 1:5,000 scale T-Sheets and the USGS 1:24,000 scale topographic maps. Shorelines thus derived can be used in a variety of coastal applications.

ACKNOWLEDGEMENTS

This research is supported by the Digital Government Program of the U.S. National Science Foundation.

REFERENCES

- Di, K., R. Ma and R. Li, 2001. Deriving 3-D shorelines from high resolution IKONOS satellite images with rational functions. In: *Proc. ASPRS Annual Convention*, St. Louis, MO (CD-ROM).
- Di, K., R. Ma and R. Li, 2003a. Rational functions and potential for rigorous sensor model recovery. *Photogramm. Eng. Remote Sens.*, 69(1), pp. 33-41.
- Di, K., R. Ma and R. Li, 2003b. Geometric processing of IKONOS Geo stereo imagery for coastal mapping applications. *Photogramm. Eng. Remote Sens.*, 69(8), pp. 873-879.
- DigitalGlobe, 2002. QuickBird Imagery Products – Product Guide. DigitalGlobe, Inc. [http://www.digitalglobe.com/downloads/QuickBird Imagery Products - Product Guide.pdf](http://www.digitalglobe.com/downloads/QuickBird%20Imagery%20Products%20-%20Product%20Guide.pdf) (accessed 27 April, 2004)
- Fraser, C. S., and Hanley, H. B., 2003. “Bias compensation in rational functions for IKONOS satellite imagery.” *Photogramm. Eng. Remote Sens.*, 69(1), pp. 53-57.
- Grodecki, J. and G. Dial, 2003. Block adjustment of high-resolution satellite images described by rational polynomials. *Photogramm. Eng. Remote Sens.*, 69(1), pp. 59-68.
- Li, R., 1998. “Potential of high-resolution satellite imagery for national mapping products.” *Photogramm. Eng. Remote Sens.*, 64(2), pp. 1165-1169.
- Li, R., K. Di, G. Zhou, R. Ma, T. Ali, and Y. Felus, 2001. Coastline mapping and change detection using one-meter resolution satellite imagery. Project Report submitted to Sea Grant/NOAA, 146 pp.
- Li, R., K. Di and R. Ma, 2003. 3-D shoreline extraction from IKONOS satellite imagery. *Marine Geodesy*, 26(1/2):107-115.
- Space Imaging, LLC. 2002. IKONOS Imagery Products – Product Guide. http://www.spaceimaging.com/whitepapers_pdfs/IKONOS_Product_Guide.pdf (accessed 27 April, 2004)
- Tao, C.V. and Y. Hu, (2001). A comprehensive study of the rational function model for photogrammetric processing. *Photogramm. Eng. Remote Sens.*, 67(12), pp. 1347-1357.
- Toutin, T., (2003). “Error tracking in IKONOS geometric processing using a 3D parametric model.” *Photogramm. Eng. Remote Sens.*, 69(1), pp. 43-51.
- Zhou, G. and R. Li, (2000). Accuracy evaluation of ground points from IKONOS high-resolution satellite imagery. *Photogramm. Eng. Remote Sens.*, 66(9), pp. 1103-1112.